Journal of Physiology (1988), **398**, *pp.* 475–505
With 12 text-figures
Printed in Great Britain

VOLTAGE SENSORS OF THE FROG SKELETAL MUSCLE MEMBRANE REQUIRE CALCIUM TO FUNCTION IN EXCITATION–CONTRACTION COUPLING

BY GUSTAVO BRUM*, ROBERT FITTS†, GONZALO PIZARRO AND EDUARDO RÍOS

From the Department of Physiology, Rush University, School of Medicine, 1750 West Harrison Street, Chicago, IL 60612, U.S.A.

(*Received 8 May 1987*)

SUMMARY

1. Intramembrane charge movements and changes in intracellular Ca^{2+} concentration (Ca^{2+} transients) elicited by pulse depolarization were measured in frog fast twitch cut muscle fibres under voltage clamp.

2. Extracellular solutions with very low [Ca^{2+}] and 2 mM-Mg^{2+}, shown in the previous paper to reduce Ca^{2+} release from the sarcoplasmic reticulum (SR), were found to cause two changes in charge movement: (a) a decrease (-12 nC/μF) in the charge that moves during depolarizing pulses from -90 to 0 mV, termed here 'charge 1'; (b) an increase ($+7$ nC/μF) in the charge moved by hyperpolarizing pulses from -90 to -180 mV, termed 'charge 2'.

3. The increase in charge moved by hyperpolarizing pulses was correlated ($r = 0{\cdot}64$) with the decrease in charge moved by depolarizing pulses and both were correlated with the inhibition of Ca^{2+} release recorded in the same fibres.

4. The low Ca^{2+} solutions caused a shift to more negative voltages of the dependence relating charge movement and holding potential (V_H). This shift is of similar magnitude (about 22 mV) and direction as the shift in the curve relating Ca^{2+} release flux to V_H (previous paper).

5. In solutions with normal [Ca^{2+}] a conditioning depolarization to 0 mV, of 2 s duration, placed 100 ms before a test pulse from -70 to 0 mV, reduced by 30% the amount of charge displaced by the test pulse. Conditioning pulses of 1 s or less caused potentiation of charge movement by up to 30%.

6. In low Ca^{2+} solutions, reduction of charge was observed at all durations of the conditioning pulse. The duration for half-inhibition was near 200 ms.

7. An extracellular solution with no metal cations caused a more radical inhibition than the low Ca^{2+} solutions that contained Mg^{2+}. The inhibition of Ca^{2+} release was essentially complete (90–100%). The charge moved by a pulse to 0 mV was reduced by 20 nC/μF and the charge moved by a pulse to -170 mV increased 8 nC/μF. This shows that Mg^{2+} supports excitation–contraction (E–C) coupling to some extent.

* Present address: Departamento de Biofísica, Facultad de Medicina, Montevideo, Uruguay.
† Permanent address: Department of Biology, Marquette University, Milwaukee, Wisconsin, U.S.A.

8. A state model of the voltage sensor of E–C coupling explains qualitatively the observations in both papers. The voltage sensor has at least four states: a resting state, an active state, which signals the SR to release Ca^{2+}, and two inactivated states. Depolarization drives the resting → active transition and moves charge 1. When the depolarization is maintained the system goes to inactivated states; changes in potential drive transitions between these and cause a charge movement with very different properties (charge 2).

9. In this model Ca^{2+} has high affinity for the resting and active states and low affinity for the inactivated states. Low $[Ca^{2+}]_o$, as well as prolonged depolarization, favour the inactivated states, diminish charge 1 and Ca^{2+} release, and increase charge 2. In the total absence of Ca^{2+} and Mg^{2+} the system is inactivated even at normal resting potentials.

10. The observations support the concept that a large portion of intramembrane charge movement originates at the voltage sensor of excitation–contraction coupling.

INTRODUCTION

In the first paper of this series (Brum, Ríos & Stéfani, 1988) we described effects of low external calcium ion concentrations ($[Ca^{2+}]_o$) on the release of Ca^{2+} from the sarcoplasmic reticulum (SR) measured in muscle fibres under voltage clamp.

We gave evidence that these effects are exerted by Ca^{2+} from the exterior of the cell and therefore suggested that the effect of $[Ca^{2+}]_o$ on calcium release is mediated by alterations in the voltage-sensing structures of the T-tubular membrane.

These structures are believed to produce 'intramembrane charge movement' when undergoing voltage-driven conformational changes that somehow control the SR Ca^{2+} channels (Schneider & Chandler, 1973). In the present paper we turn to studying the effects of low $[Ca^{2+}]_o$ on intramembrane charge movement. In all the experiments we simultaneously monitor Ca^{2+} release from the sarcoplasmic reticulum (Melzer, Ríos & Schneider, 1984, 1987; Brum *et al.* 1988).

The general inhibition of Ca^{2+} release by low $[Ca^{2+}]_o$ reported in the previous paper has three related aspects: a reduction in the peak Ca^{2+} release flux, an enhancement of the rate of inactivation of release during a depolarizing pulse, and a shift of the steady-state inactivation curve of release *versus* holding potential (V_H) to more negative potentials.

All these effects can be explained by corresponding effects on charge movement. The charge that moves in the voltage range in which Ca^{2+} release is activated is less in low $[Ca^{2+}]_o$, diminishes (is immobilized) more rapidly during a depolarizing pulse in low $[Ca^{2+}]_o$, and its equilibrium inactivation curve is shifted to more negative holding potentials. All the observations on release are thus explicable as effects of Ca^{2+} on charge movement.

Additionally, low $[Ca^{2+}]_o$ causes a rather unexpected effect: it increases the magnitude of charge movement in a very negative voltage range. We have previously shown (Brum & Ríos, 1987) that a similar phenomenon occurs in fibres held at 0 mV for a minute or more, a finding recently confirmed by Melzer & Pohl (1987). In those fibres, which are called 'inactivated' or 'refractory' (because they cannot release Ca^{2+}), the charge that moves at very negative voltages (−100 to −200 mV) is

increased, while charge that moves in the normal activating range of voltage (−70 to 30 mV) disappears. Accordingly, the observed increase of charge movement in the range −100 to −200 mV in low $[Ca^{2+}]_o$ is interpreted here as evidence that low Ca^{2+} drives the fibres into partial inactivation.

Most effects of $[Ca^{2+}]_o$ on charge movement may be explained by a simple state model of the voltage sensor (Brum & Ríos, 1987) together with the postulate that Ca^{2+} is normally bound to a site on the voltage sensor and must dissociate from it to permit inactivation.

This work thus provides insights into the mechanism of inactivation; additionally, it suggests a straightforward explanation of the recently described inhibitory effects of Ca^{2+} channel blockers on Ca^{2+} release and intramembrane charge movement (Hui, Milton & Eisenberg, 1984; Ríos & Brum, 1986, 1987; Lamb, 1987; Berwe, Gottschalk & Lüttgau, 1987; Lüttgau, Gottschalk & Berwe, 1987; Melzer & Pohl, 1987).

Finally, this work amounts to a comprehensive comparison of intramembrane charge movement and Ca^{2+} release under many conditions. A very good correlation between the size and time course of charge movement and release holds in spite of wide changes of both, strongly supporting the view that most of intramembrane charge movement arises at the voltage sensor of E–C coupling.

METHODS

The experiments were performed in cut skeletal muscle fibres of the frog (*Rana pipiens*) under voltage clamp. The methods for dissection and mounting of the fibre, as well as for determination of the time course of change in myoplasmic $[Ca^{2+}]_o$ (Ca^{2+} transients) and the time course of Ca^{2+} release from SR, were described in the first paper of this series (Brum *et al.* 1988). Intramembrane charge movement current (I_Q) was determined by two methods: (1) A conventional method, in which charge movement is calculated by adding the current recorded during a depolarizing (test) pulse to the scaled current recorded during a hyperpolarizing (control) pulse from the same holding potential. The details of this method are as described by Horowicz & Schneider (1981*a*). (2) An alternative analysis of charge movement was also used. This method was introduced in a previous paper (Brum & Ríos, 1987). It differs from the conventional method in the definition of control pulses for subtraction of linear capacitive components of the total current. In this procedure the control current is recorded in the fibre held at 0 mV, using a depolarizing pulse to +80 mV. The justification of this method is simply that the controls constructed in this way fully satisfy the required properties of linearity (Brum & Ríos, 1987). This method involves differences between currents obtained at different times; to minimize the problem posed by slow changes in linear capacitance observed sometimes during the experiment (Brum & Ríos, 1987) controls were recorded before and after most runs of test pulses. In all fibres linearity in total current in the control range of voltages was explored by applying small (20 mV) pulses starting from a level ranging from 0 to 80 mV. If no difference was found in the currents elicited by the small pulses, the full range 0–80 mV was used for determination of control currents. In two of twelve fibres and towards the end of the experiments evidence of non-linear ionic currents (probably due to fibre decay) was found at potentials beyond +60 or +70 mV. In those cases the control currents were generated by pulses to +50 or +60 mV.

Solutions

The internal and external solutions, designed to minimize ionic currents, were the same as in the previous paper (Brum *et al.* 1987). The internal solution was essentially an isotonic caesium glutamate with 0·8 mM-Antipyrylazo III for the determination of Ca^{2+} transients. The external solutions were all variants of the reference solution with different concentrations of Ca^{2+}. We used a 10 μM-Ca^{2+} solution (buffered with 30 mM-HEDTA) and a 0 Ca^{2+} solution (with 5 mM-EGTA and no added Ca^{2+}). These low Ca^{2+} solutions had 3 mM-Mg^{2+} added and a free $[Mg^{2+}]$ of 2·4 mM.

Another low Ca^{2+} solution (0 Ca^{2+} 0 Mg^{2+}) had the same composition as the reference solution but no Ca^{2+} (or Mg^{2+}) added; it also contained 0·5 mM-EGTA. Finally, in one series of experiments 1 mM-Ca^{2+} and 10 mM-Ca^{2+} were also used (Table 1, previous paper).

RESULTS

Conventional measurement of intramembrane charge

Figure 1 shows records of intramembrane charge movement in a fibre exposed to reference solution (panel *A*) and 10 μM-Ca^{2+} (panel *B*). The records were obtained by

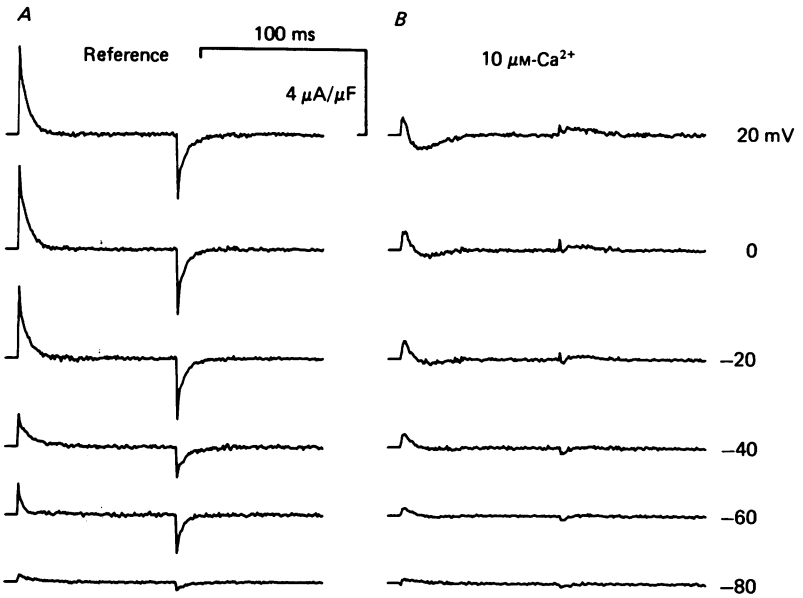

Fig. 1. Intramembrane charge movements measured conventionally. Records obtained by subtraction of a scaled 'control' current from 'test' currents measured during 100 ms pulses from a holding potential of −100 mV to the potential indicated next to the records. The control currents were measured during hyperpolarizing pulses to −160 mV. Only the 'off's of the control currents were used. Both the control currents and the test-minus-scaled control records were corrected for sloping baselines fitted between 51 and 100 ms during the transient. *A*, reference external solution. *B*, 10 μM-Ca^{2+} solution. Temperature, 7 °C. Fibre diameter, 70 μm. The linear capacitance measured from the controls in reference solution was 9·94 nF (in a fibre segment of 540 μm this corresponds to 8·35 μF/cm^2 of fibre surface area). The vertical bar thus corresponds to about 40 nA. The control records in 10 μM-Ca^{2+} gave a capacitance of 12·06 nF or 20% greater than in reference solution. Fibre 123.

the conventional method of subtracting a scaled 'control' from the current recorded with the 'test' pulse. The control records were obtained with −40 mV pulses from the holding potential of −100 mV. The left-hand records have the usual characteristics of charge movements in cut fibres. However, the records in low Ca^{2+} have in most cases a slow component with polarity opposite to that of a capacitive current, which means that something in the method has gone wrong.

A simple explanation of the paradoxical records in Fig. 1*B* is that there is charge movement in the so-called controls; at times later than 10 ms during the pulse this

charge becomes proportionally greater in the controls than in the test pulses, resulting in 'negative charge' in the difference records.

Alternative measurement of intramembrane charge

To look for charge movement in the voltage range negative to −100 mV it was convenient to define controls of linear capacitance in an alternative way, which did

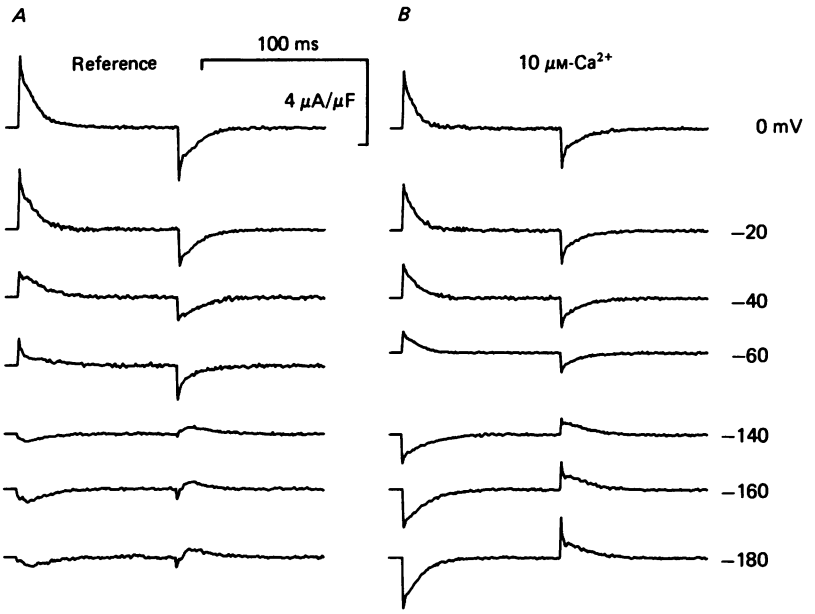

Fig. 2. Intramembrane charge movements with alternative controls. Same fibre and records as in Fig. 1 except that the control currents were measured when the fibre was held at $V_H = 0$ mV with pulses to +80 mV. The linear capacitance measured from the control records was 9·2 nF or 7·73 μF/cm² of fibre surface. Accordingly, the calibration bar (40 nA) corresponds to 4·35 μA/μF if the alternative controls are used as measure of linear capacitance, or to 4 μA/μF if the conventional controls are used.

not assume the non-existence of charge movements in the negative voltage range. In previous work (Brum & Ríos, 1987) it was shown that the capacitance of the membrane of a fibre held at 0 mV was remarkably constant and *minimum* at voltages positive to 0 mV.

In the present work we took advantage of this observation by using current records, obtained with positive pulses (to +80 mV) while the fibres were held at 0 mV, as measures of linear capacitance. Routinely, the experiments were started from a depolarized situation ($V_H = 0$ mV), controls were recorded, then the fibre was polarized ($V_H = -100$ mV), pulses to several test potentials were applied, then the holding potential was again taken to 0 mV and bracketing controls obtained.

The records in Fig. 2 are membrane charge movements constructed with the alternative controls and the same test currents as in Fig. 1. In this and ten other fibres (Table 1) the following observations were made. There is non-linear (asymmetric) current during pulses to voltages negative to −100 mV in all cases, in all external solutions. The asymmetric current during the negative-going pulses was

greater in low $[Ca^{2+}]_o$ in ten fibres out of eleven, although the difference was variable. The asymmetric current (charge movement) during positive-going pulses was less in low $[Ca^{2+}]_o$ in ten fibres.

In Fig. 3 we plotted the areas under the asymmetric current records for both the 'on' transients (□, ■) and the 'off' transients (○, ●) in reference solution (○, □)

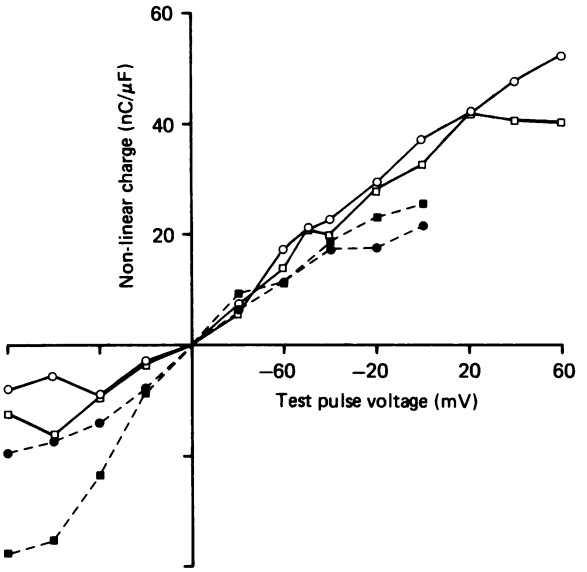

Fig. 3. Voltage dependence of asymmetric charge. Charges displaced by the transient currents in Fig. 2 (areas under the curves). Open symbols, reference solution; filled symbols, 10 μM-Ca^{2+}. Squares, 'on' charges; circles, 'off' charges.

and 10 μM-Ca^{2+} (●, ■). The main observation is that positive-going pulses displace less charge in low $[Ca^{2+}]_o$ and the opposite occurs with hyperpolarizing pulses. This result does not depend on the fact that the records in the Figure were constructed using a non-conventional control; even though the records shown do depend on the choice of control, the differences induced by the low $[Ca^{2+}]_o$ do not, as the control current was the same for all records shown.

In both solutions the areas of the transients tend to saturate at both extremes of voltage. However, at large negative voltages the 'on' area is greater than the 'off'; whereas at large positive voltages the opposite difference occurs. Major differences between 'on' and 'off' areas are an indication of residual ionic currents. At the extreme of high positive voltages an excess of 'off' over 'on' area was first shown by Horowicz & Schneider (1981*a*) who also showed that it disappeared in an external solution with Co^{2+}, which is consistent with the excess 'off' area being a deactivation ('tail') current flowing through a Ca^{2+}channel opened by the large pulses. These tails are not observed in our low Ca^{2+} solutions.

Analogously, the excess 'on' area during large hyperpolarizing pulses, first shown by Brum & Ríos (1987), was interpreted as a deactivation tail current through channels open at the holding potential, that close upon hyperpolarization. This ionic current may be eliminated by two methods (Brum & Ríos, 1987): external solutions

containing EGTA (which suggests that the current is carried by Ca^{2+} or through Ca^{2+}-activated channels), or a large negative conditioning pulse as shown in Fig. 4.

The two records of Fig. 4*A* are 'charge movement' transients obtained in reference solution with a pulse to −20 mV (pulse A in inset). The two records in Fig. 4*B* were obtained with a pulse to −160 mV (B in inset). The records represented as a point

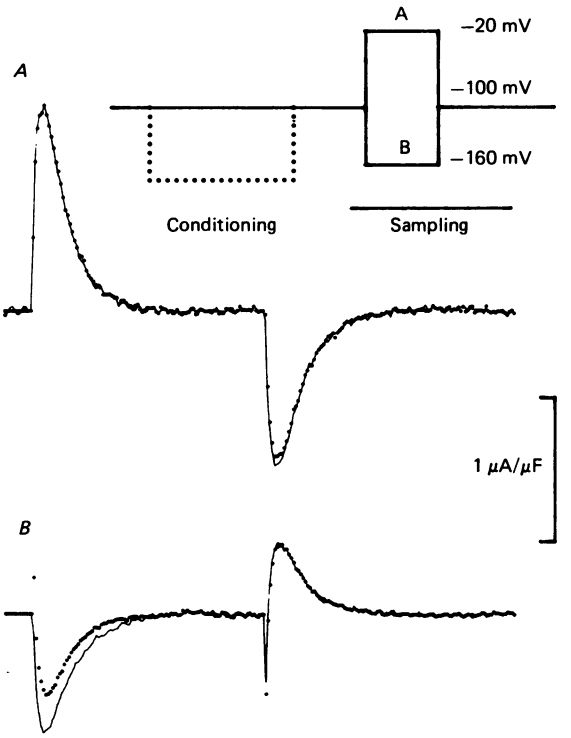

Fig. 4. Effect of a hyperpolarizing conditioning pulse on asymmetric currents. Differences between test records, measured during test pulses to −20 mV (A) or −160 mV (B) from $V_H = -100$ mV, and scaled control records measured in the fibre held at $V_H = 0$ mV during pulses to +80 mV. A conditioning pulse of 200 ms duration to −180 mV (dotted line in inset) was intercalated, ending 100 ms before the test pulses. Point plots: records with conditioning pulse applied; line plots, no conditioning pulse applied. Reference solution. Temperature, 11 °C. Fibre diameter, 63 μM. Linear capacitance, 7·43 nF or 7·29 μF/cm² of fibre surface. Vertical bar, 7·43 nA. Fibre 207.

plot were obtained when the test pulse was preceded by a 200 ms pulse to −190 mV (dotted in inset). The large negative conditioning pulse in *B* reduced the 'on' transient without changing the 'off' transient. Without the conditioning pulse, the area under the 'on' transient was substantially larger than that under the 'off' transient. With the pulse, the areas became equal; presumably the conditioning pulse closed the channels and the 'on' and 'off' transients became equal. This is an indication that what is measured when a large negative pulse is applied before the test pulse is pure charge movement.

Remarkably, the 'off' of the record in *B* is not modified by the conditioning pulse. This is an interesting observation because it allows us to estimate the charge movement as the area of the 'off' in the many cases in which a fibre cannot tolerate

a large conditioning pulse preceding every test pulse. In *A*, the conditioning pulse had no major effect, indicating that the ionic current is not time dependent at potentials positive to −100 mV. Consequently, there are no ionic components in the asymmetric current transient during the trailing edge of a hyperpolarizing pulse.

The fact that this inward ionic current is large in the 10 μM-Ca^{2+} solution is evidence that Mg^{2+}, present in the solution at a concentration of 2·4 mM, may carry

TABLE 1. Changes in charge movement and Ca^{2+} release in low $[Ca^{2+}]_o$

	A	B	C	D	E	F	
	Charge at 0 mV (nC/μF)			Charge at −180 mV (nC/μF)			Inhibition of Ca^{2+}
Fibre	Reference	Low Ca^{2+}	A–B	Reference	Low Ca^{2+}	D–E	release
111	40·2	7·0	33·2	−17·1	−35·2	18·1	0·99
112	24·7	11·5	13·2	−3·0	−11·6	8·6	0·22
113	23·9	19·4	4·5	−6·9	−8·9	2·0	0·19
114	30·4	16·5	13·9	−9·3	−31·0	21·7	0·73
119	34·0	35·3	−1·3	−6·1	−6·8	0·7	0·12
123	37·3	25·6	11·7	−8·2	−19·6	11·4	0·80
126	19·0	9·9	9·1	−7·8	−14·1	6·3	0·39
134	41·9	35·8	6·1	−6·3	−5·4	−0·9	—
168	18·4	5·0	13·4	−12·2	−17·8	5·6	1·00
168A	30·4	14·8	15·6	−11·0	−11·6	0·6	0·15
262	30·5	18·3	12·2	−13·7	−17·0	3·3	—
Average	30·06	18·10	11·96*	−9·23	−16·27	7·04*	0·51*
(S.E.M.)	(2·40)	(3·14)	(2·60)	(1·20)	(2·86)	(2·23)	(0·12)

All fibres were exposed sequentially to reference solution and a low Ca^{2+} solution (either 0 Ca^{2+} or 10 μM-Ca^{2+}). The fibres were at holding potentials of −100 or −90 mV, and, in one case (fibre 126) at −75 mV. Pulses were applied from the holding potential to 0 or −180 mV. The charge displaced by those pulses was evaluated after subtraction of a control current obtained in the same fibres at a holding potential of 0 mV. For the hyperpolarizing case, charge was evaluated by the 'off' area of the asymmetric current. For the depolarizing pulse the 'on' area was used (rationale in text). Note that, for simple conventional reasons, the charges displaced by hyperpolarizing pulses are listed as negative. An analysis of the paired differences $C-F \equiv A+|D|-(B+|E|)$, that is the difference between total charge in reference solution and total charge in low $[Ca^{2+}]_o$, gave an average of 4·93 nC/μF (a significant increase, $P < 0.05$). Inhibition of Ca^{2+} release (last column) was calculated as: (peak Ca^{2+} release flux in reference − peak Ca^{2+} release flux in low Ca^{2+})/peak release in reference solution. Dashes, no measurement taken. * Significant change, $P < 0.01$.

this current. We have confirmed this observation in studies at $V_H = 0$, a condition that makes this current large (G. Brum, E. Ríos & E. Stéfani, unpublished observations).

Based on these observations we used the 'off' areas to measure the charge moved with hyperpolarizing pulses. The charge in depolarizing pulses was estimated as average of 'on' and 'off' below 0 mV and by the 'on' only at or beyond 0 mV.

Table 1 summarizes the observations on the magnitude of charge movement with depolarizing and hyperpolarizing pulses in reference and low $[Ca^{2+}]_o$ (either 0 Ca^{2+} or 10 μM-Ca^{2+}). Columns A and B list charge moved by a pulse to 0 mV (from a V_H of −90 or −100 mV). Columns D and E list charge moved by a pulse to −180 mV from the same holding potential. The Table also lists the differences: Q in reference $-Q$ in low Ca^{2+} (columns C and F). In all but one of the fibres low Ca^{2+} caused a decrease

of the charge moved by the depolarizing pulse. In all but one the charge moved by the hyperpolarizing pulse increased. Both average changes were significantly different from 0 ($P < 0.001$). The changes (columns C and F), had a correlation coefficient of 0·64.

A possible interpretation of the reciprocal changes induced by low $[Ca^{2+}]_o$ in the charges moved by pulses of opposite polarity is that low $[Ca^{2+}]_o$ causes a simple shift to the left of the Q *vs.* V distribution, without changing total mobile charge. In a paired t test the reduction due to low Ca^{2+} in charge moved by the depolarizing pulse was significantly greater than the increase in charge moved by the hyperpolarizing pulse ($P < 0.05$); in other words, not all the charge that disappeared in low Ca^{2+} in the voltage range positive to V_H appeared in the negative voltage range. This is confirmed by other results presented below (Fig. 9).

Effects of low $[Ca^{2+}]_o$ on Ca^{2+} release

As shown in the previous paper, low Ca^{2+} solutions cause a reduction of variable magnitude in Ca^{2+} release flux. We compare in Table 1 this effect with the effects on charge movement, by listing in the last column a measure of the inhibition of peak release flux (R_p) calculated as (R_p in reference $- R_p$ in low Ca^{2+})/R_p in reference. Large changes in charge were generally associated with large inhibitions of release. The correlation coefficient between the change in charge moved by depolarizing pulses (column D) and inhibition of release was 0·631. The correlation coefficient between the increase in charge moved by hyperpolarizing pulses and inhibition of release was 0·682. Correlation coefficients near 0·65 for $n = 11$ have a high significance ($P < 0.02$, Winkler & Hays, 1975). Summing up, the inhibition of Ca^{2+} release is well correlated with both types of changes in the distribution of mobile charge, which in turn are well correlated mutually.

Low $[Ca^{2+}]_o$ changes steady-state inactivation

A remarkable effect of low Ca^{2+} on release is a shift to the left of the curve relating release to holding potential (inactivation curve) by some 29 mV (Brum *et al.* 1988). We performed similar experiments to determine inactivation curves for charge movement. The pulse protocol and results are represented in Fig. 5. The independent variable in the measurements is V_H, which varied from -90 to 0 mV in steps of 10 mV. Charge was measured during a test pulse spanning the -70 to 0 mV range (that is, a pre-pulse of 100 ms always took the potential to -70 mV before the test pulse to 0 mV). The rationale of having such a pre-pulse is to avoid the negative voltage range in which charge 2 moves in depolarized fibres (Brum & Ríos, 1987) and mobile charge increases in low Ca^{2+} as shown in the previous section; by exploring the charge mobile in a more positive voltage range we expected, and found, a purely inhibitory effect of prolonged depolarization.

To permit a collective plot of data from several fibres the values in the graph are normalized to the value measured at $V_H = -90$ mV; open symbols correspond to reference solution and closed symbols to results in 10 μM-Ca^{2+}. The continuous curve was generated with the function,

$$Q_\infty + (1 - Q_\infty)/\{1 + \exp[(V_H - \bar{V}_H)/k]\}, \quad (1)$$

a sigmoidal function centred at $\bar{V}_H$ with a limiting value Q_∞ at high V_H. The effect of low $[Ca^{2+}]_o$ was to shift the curve to more negative potentials by about 22 mV. As shown in the previous paper (Brum *et al.* 1988) the inactivation curve of Ca^{2+} release flux is shifted by −29 mV in low $[Ca^{2+}]_o$. The difference between both shift values is within the error of their estimates. This parallel shift of similar magnitude is

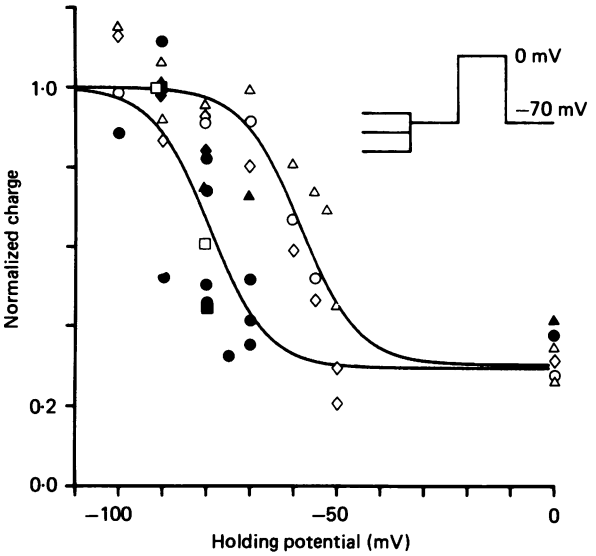

Fig. 5. Steady-state inactivation of intramembrane charge movement. Charge moved by a pulse to 0 mV in fibres held for 3 min or longer at the potential in the abscissa. The potential was brought to −70 mV (inset) for 100 ms before the test pulse. The charges were normalized to their average value at the holding potential of −100 and −90 mV. Open symbols, reference solution; closed symbols, low Ca^{2+}. Fibres 244 (□), 252 (○), 254 (△), 255 (◇). Temperatures: 11, 11, 11 and 9 °C, respectively. The curves were generated with eqn (1) best fit to the data. The best-fit parameter values in reference solution were: $Q_\infty = 0{\cdot}301$, $\bar{V}_H = -58{\cdot}1$, $k = 6{\cdot}66$. In low Ca^{2+}: $Q_\infty = 0{\cdot}293$, $\bar{V}_H = -80{\cdot}1$, $k = 6{\cdot}57$.

most simply interpreted as due to a causal relationship; low $[Ca^{2+}]_o$ primarily shifts the inactivation curve of charge movement – less charge moves at a given V_H – consequently, less Ca^{2+} is released.

The rate of charge immobilization is increased in low Ca^{2+}

The experiments in this section were again inspired by observations on Ca^{2+} release. We showed in the previous paper that the release flux waveform decays more rapidly during a depolarizing pulse in low $[Ca^{2+}]_o$ than in reference solution. This would be expected if low $[Ca^{2+}]_o$ caused the inactivation of intramembrane charge, known to occur during prolonged depolarization (Chandler, Rakowski & Schneider, 1976), to develop more rapidly. In turn, this would explain the left-shift in the inactivation curve seen in the previous section, as an enhancement in the rate of (voltage-dependent) inactivation, which results in a greater steady-state inactivation at a given V_H.

Inactivation of charge during a depolarizing pulse (commonly referred to as 'charge immobilization' in the case of channel gating currents; Armstrong &

Bezanilla, 1977) may be studied by evaluating the difference between 'off' and 'on' during pulses of increasing duration. This procedure is impractical here due to the parallel activation of Ca^{2+} channels during long depolarizing pulses, because open Ca^{2+} channels contribute large tails at the 'off' obscuring charge movement. A more convenient alternative is shown in the inset of Fig. 6. A conditioning pulse of variable

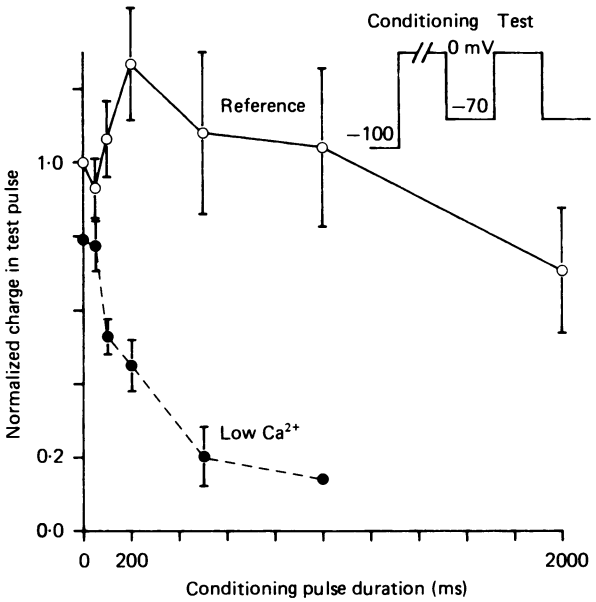

Fig. 6. Charge inactivation by a conditioning pulse. A conditioning pulse of variable duration, to 0 mV, was applied ending 100 ms before a test pulse to 0 mV (inset). The charge displaced by the test pulse is plotted as a function of conditioning pulse duration. The values of charge are averages of 'on' and 'off' normalized to the unconditioned value in reference solution. The vertical bars span standard errors of the mean over four fibres. Not all durations were explored in all fibres. Open symbols, reference solution; closed symbols, same fibres in 10 μM-Ca^{2+}. The point at 1000 ms in 10 μM-Ca^{2+} corresponds to a single experiment. Fibres 246, 247, 248 and 249. Temperatures, between 9 and 11 °C.

duration is placed before the test pulse and the charge moved during the test pulse is evaluated. As shown in the inset, the test pulse spans the −70 to 0 mV range. A typical result is shown in Fig. 6 where charge is plotted *vs.* duration of the conditioning pulse. In reference solution (open symbols) the effect of the conditioning pulse is characteristically biphasic: at intermediate durations (100–500 ms) there is usually a potentiation, an increase in the 'on' and 'off' areas as compared with the unconditioned situation (abscissa = 0 in the plot). This unexpected result was present in all six fibres studied. Although we have not ruled out changes in ionic currents, this effect is probably a true potentiation of charge movement (as it is present both in the 'on' and the 'off' of the test pulse). Longer pulses (1 s or more) caused an inhibition of charge and half-inhibition was not achieved with conditioning pulses up to 2 s in duration. The large conditioning pulses cause a large Ca^{2+} transient. The observed potentiation of charge movement could be due to the increase in Ca^{2+} rather than the pulse *per se*. Some mechanisms by which the

intracellular Ca^{2+} transient could increase charge movement have been discussed by Horowicz & Schneider (1981*b*); another is considered in the Discussion.

In low Ca^{2+} the situation was sharply different. The unconditioned record had already less charge, and all conditioning pulses caused inhibition, with a duration for half-inhibition of between 100 and 200 ms (closed symbols).

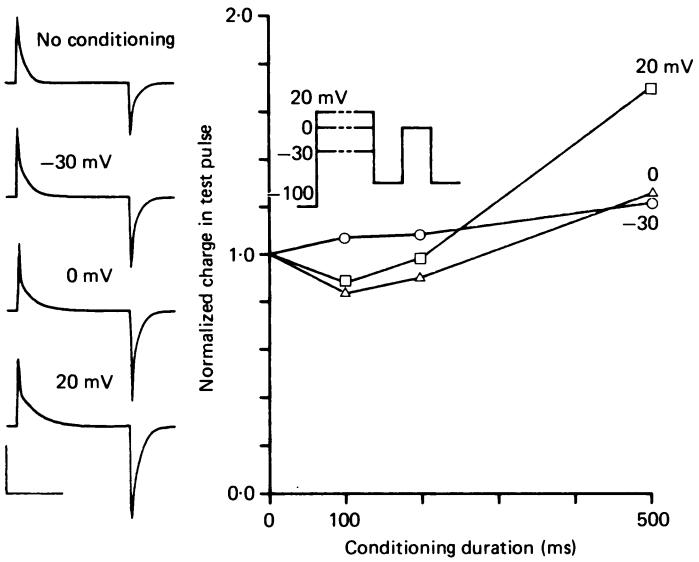

Fig. 7. Effect of conditioning pulses of variable voltage. The experiment of Fig. 6 was repeated, varying the amplitude of the conditioning pulse, as well as its duration (inset). The values plotted are charges displaced during the 'on' of the test pulse, normalized to the charge displaced by the unconditioned test pulse, *vs.* the conditioning pulse duration. ○, conditioning pulse to −30 mV; △, to 0 mV; □, to 20 mV. Holding potential, −100 mV. The test pulse went from −70 mV to 0 mV. Solution, 10 mM-Ca^{2+}. Temperature, 11 °C. Fibre diameter, 80 μm. The individual records correspond to charge transients during the unconditioned test pulse and with conditioning pulses of 500 ms to −30, 0 and 20 mV, respectively. Horizontal bar, 50 ms. Vertical bar, 50 nA or 4·69 μA/μF in a fibre of 10·66 nF of linear capacitance (8·46 μF/cm^2 of fibre surface). Fibre 242.

This is an important result; it explains the increased rate of inactivation of release during a pulse observed in low $[Ca^{2+}]_o$ as a simple consequence of increased rate of charge inactivation during the pulse. It also implies that in low $[Ca^{2+}]_o$ even a standard 100 ms duration pulse will cause substantial inactivation of charge, so that measureably less charge should move during the 'off'. This prediction was verified in all experiments in low Ca^{2+}. The records during 100 ms depolarizing pulses have always a greater area at the 'on' than the 'off' (the records in Fig. 2*B* and corresponding plot in Fig. 3 constitute typical examples).

Voltage dependence of the rate of charge immobilization

There is a trivial explanation of the effect of low $[Ca^{2+}]_o$ on the kinetics of charge inactivation. Calcium ions in the extracellular fluid could simply bind to fixed negative charges thereby making the microscopic transmembrane potential

difference more negative and shifting all curves to higher values of the macroscopic transmembrane potential. According to this hypothesis, it should be possible to cause an inhibition in reference solution just by increasing the amplitude of the conditioning depolarization. A 200 ms pulse to 0 mV causes more than 50% reduction in charge movement in low $[Ca^{2+}]_o$ (Fig. 6). A similar conditioning pulse causes a potentiation in reference solution (Fig. 6, continuous line). The experiment of Fig. 7 is a variant of the series in Fig. 6 in which the amplitude of the conditioning pulse was varied, as well as its duration (pulses in inset). The Figure plots charge moved by the test pulse as a function of conditioning pulse duration. The three different sets of points correspond to conditioning pulses to −30, 0 and 20 mV. Pulses of 200 and 500 ms are seen to cause potentiation, the pulse to +20 mV simply causing more potentiation instead of the inhibition predicted by the surface charge–binding hypothesis. This type of experiment was performed in three fibres with similar results.

The absence of divalent cations causes complete inactivation

The experiments in the previous sections were designed with the purpose of reducing $[Ca^{2+}]_o$ while maintaining the ability of the external solution to screen (in the sense of diffuse double-layer theory; McLaughlin, Szabo & Eisenman, 1971; McLaughlin, 1977) negative charges of the membrane outer surface. For this purpose the low Ca^{2+} solutions had 2·4 mM-free $[Mg^{2+}]$.

Lüttgau & Spiecker (1979) have shown that Mg^{2+} may restore K^+ contractures inhibited in low Ca^{2+} media; therefore it seemed important to study charge movement and Ca^{2+} release in solutions having neither Ca^{2+} nor Mg^{2+}. We found a dramatic effect: the absence of divalent cations caused a complete inactivation, as demonstrated in the experiments of Figs 8–10.

Parts *A* and *B* of Fig. 8 correspond to two different fibres which were exposed sequentially to reference solution, then to 0 Ca^{2+} 0 Mg^{2+}, then back to reference. Records 1 and 2 are Ca^{2+} transients in reference and in 0 Ca^{2+} 0 Mg^{2+}, respectively. For both fibres the record in reference solution was obtained after the record in 0 Ca^{2+} 0 Mg^{2+}. Records 3 and 4 are the corresponding Ca^{2+} release fluxes derived from records 1 and 2 by the techniques described in the previous paper. The 0 Ca^{2+} 0 Mg^{2+} solution reduced the peak release flux to about one-tenth of its reference value in the fibre of panel *A* and made release undetectable in the other. In four fibres of a total of six Ca^{2+} release was totally absent in 0 Ca^{2+} 0 Mg^{2+}. In the other two fibres it was reduced to one-tenth or less of its reference value.

Figure 9 illustrates charge movements in the fibre of Fig. 8*A*. Records 1 and 2 correspond to 100 ms pulse depolarizations to 0 mV in reference solution (1) and 0 Ca^{2+} 0 Mg^{2+} (2). These are the charge movement currents corresponding to Ca^{2+} transients 1 and 2 in Fig. 8. The 0 Ca^{2+} 0 Mg^{2+} solution caused a reduction in charge from 37 nC/μF (record 1) to 12 nC/μF (2). Records 3 and 4 were obtained during hyperpolarizing pulses to −170 mV. The change moved by the hyperpolarizing pulse was 5 nC/μF in reference (3) and increased to 15·2 nC/μF in 0 Ca^{2+} 0 Mg^{2+} (4). The effects of 0 Ca^{2+} 0 Mg^{2+} are then analogous but of greater magnitude than the effects of the solutions with 2·4 mM-Mg^{2+} (Table 1). In three fibres the charge moved with a pulse to 0 mV decreased by 20·2 nC/μF (S.E.M. = 5·0) in 0 Ca^{2+} 0 Mg^{2+} and the

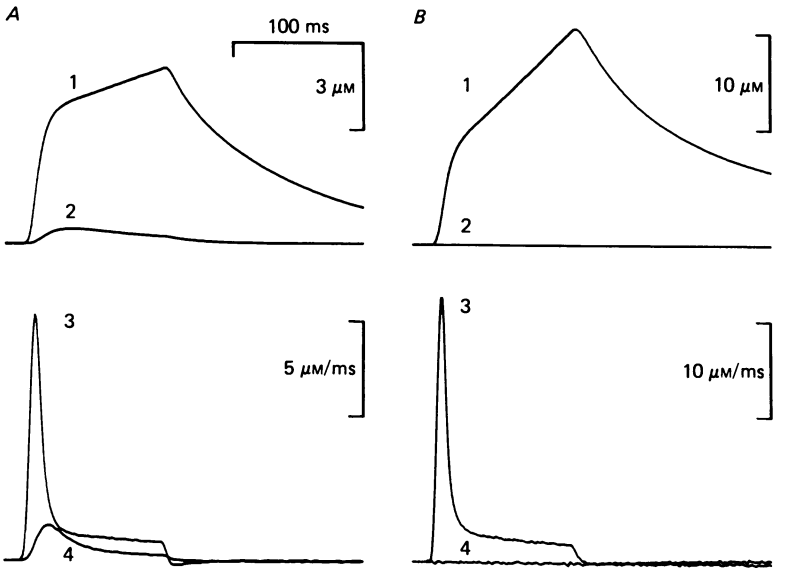

Fig. 8. Ca^{2+} transients and Ca^{2+} release in 0 Ca^{2+} 0 Mg^{2+}. *A*, fibre 235. *B*, fibre 234. The fibres were first exposed to 0 Ca^{2+} 0 Mg^{2+}, then to reference solution, at a holding potential of −90 mV. The transients were elicited by 100 ms pulses to 0 mV; all records shown are averages of two. Record 1, Ca^{2+} transient in reference solution; record 2, Ca^{2+} transient in 0 Ca^{2+} 0 Mg^{2+}. Records 3 and 4, corresponding Ca^{2+} release fluxes (there were no detectable transients or release fluxes in the fibre in *B* when it was exposed to 0 Ca^{2+} 0 Mg^{2+}). Fibre 235 (*A*): diameter, 107 μm; temperature, 9 °C; dye concentration, between 278 and 283 μM. Fibre 234 (*B*): diameter, 80 μm; temperature, 12 °C; dye concentration, between 284 and 314 μM.

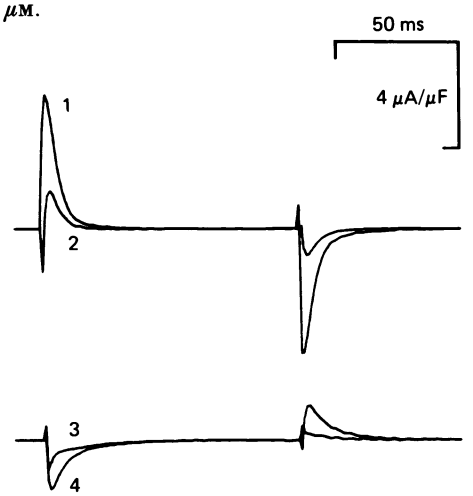

Fig. 9. Charge movements in 0 Ca^{2+} 0 Mg^{2+}. Asymmetric currents during a pulse to 0 mV (top records) or −170 mV (bottom) in a fibre exposed sequentially to 0 Ca^{2+} 0 Mg^{2+} (records 2 and 4) and reference solution (1 and 3). The membrane potential was held at −90 mV until 100 ms before the pulse, when it was changed to −70 mV; the records shown are then currents during transitions between −70 and 0 mV (top) and between −70 and −170 mV (bottom). The controls of linear capacitive current were obtained with the holding potential at 0 mV as described in Methods. Same fibre and positive pulses as in Fig. 8*A*. Fibre 235: diameter, 107 μm; linear capacitance, 20·63 nF or 9·05 μF/cm². The vertical bar, 4 μA/μF, corresponds to 82·5 nA.

charge moved by a pulse from -70 to -170 mV increased 8·0 nC/μF (S.E.M. = 3·8).

Figure 10 plots charge *vs.* test voltage for another fibre in 0 Ca^{2+} 0 Mg^{2+} at a holding potential of -100 mV. In this fibre, as in all fibres in 0 Ca^{2+} 0 Mg^{2+}, more charge moved below than above -100 mV. The continuous curves represent the two-state canonical distribution function ('Boltzmann'),

$$Q = Q_{V_H} + Q_{max}/\{1+\exp[-(V-\bar{V})/k]\}. \quad (2)$$

One of the curves was generated with best-fit least-square values of the parameters. In the other case (arrow) the curve was generated with $\bar{V} = -115$ mV and $k = 21{\cdot}5$

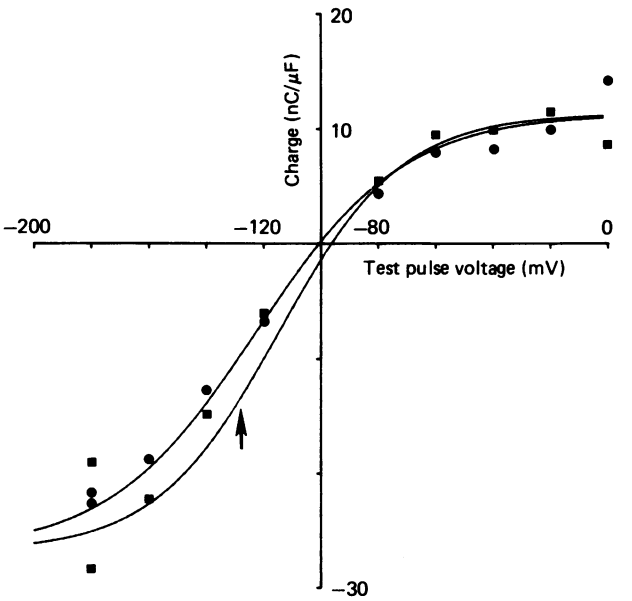

Fig. 10. Distribution of charge in a fibre in 0 Ca^{2+} 0 Mg^{2+}. Ordinate: charge displaced by 100 ms pulses to the potential in the abscissa; ■, 'on' transients; ●, 'off's. The fibre was at a holding potential of -100 mV in 0 Ca^{2+} 0 Mg^{2+}. Temperature, 10 °C. Fibre 169A. Continuous curves generated with text eqn (2). The curve going through the points is a least-squares fit with parameters $Q_{max} = 38{\cdot}116$, $\bar{V} = -122{\cdot}8$, $k = 25{\cdot}73$ and $Q_{V_H} = 26{\cdot}87$. The other curve (arrow) was generated with the same value of Q_{max}, $\bar{V} = -115{\cdot}0$ and $k = 21{\cdot}5$ which are the average parameters of the distribution of charge in depolarized fibres (Brum & Ríos, 1987).

mV which are the average best-fit values of the parameters found by Brum & Ríos (1987) for charge 2, the mobile charge of fibres being maintained at a holding potential of 0 mV. Both curves are similar and describe the data well.

The solution with no divalent cations thus induces, in normally polarized fibres, a condition analogous to the refractoriness or inactivation of a depolarized fibre. This condition includes absence of Ca^{2+} release and a characteristically altered charge movement. The inactivated condition seems to be the full expression of the effects of low $[Ca^{2+}]_o$ studied in this series of papers.

Direct comparisons between Ca^{2+} release and charge movement

The results reported in the previous sections and in the previous paper amount to the observation of remarkably parallel changes in Ca^{2+} release flux and charge movement, especially the charge movement that occurs during depolarizing pulses that start from −70 mV. It seems that, regardless of the external solution, holding potential or test potential, peak release flux is determined primarily by the quantity of charge that moves between −70 mV and the test voltage.

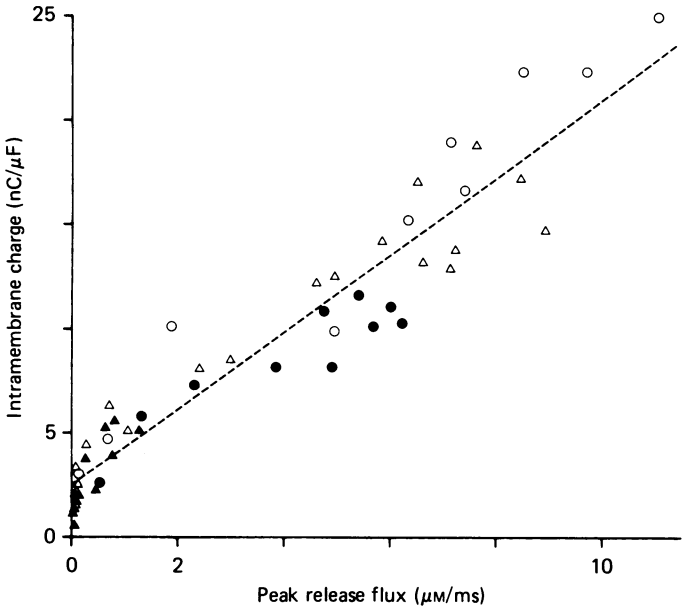

Fig. 11. Relationship between intramembrane charge movement and Ca^{2+} release. Ordinate: intramembrane charge displaced by pulses of different amplitudes, all starting from −80 mV. For pulses to less than 0 mV the averages of 'on' and 'off' are plotted. The 'on' charges are plotted for pulses to higher voltages. Abscissa: peak Ca^{2+} release flux. Open symbols, reference solution; filled symbols, 10 μM-Ca^{2+}. Circles, $V_H = -90$ mV; triangles, $V_H = -80$ mV. Fibre diameter, 101 μm. Linear capacitance, 13·62 nF (8·68 μF/cm² of fibre surface). The dashed line was obtained by linear regression to all points. The regression parameters are: Y intercept, 2·44; slope, 1·84; correlation coefficient, 0·957. Temperature, 11 °C. Fibre 244.

Figure 11 shows a thorough demonstration of this claim. Peak release flux and charge movement were determined at two holding potentials (−90 mV, circles, and −80 mV, triangles) in two external solutions (reference, open symbols, and 10 μM-Ca^{2+}, closed symbols) with pulses to different test potentials. The plot shows that, regardless of the conditions, the peak release flux is a uniform, almost linear function of the quantity of charge moved during the pulse.

The important qualification here is that the charge that moves positive to −70 mV is positively correlated with Ca^{2+} release; the charge that moves at more negative potentials is not, and in fact is negatively correlated (Table 1). In the Discussion we interpret these observations as indicating that the positive-going pulses from −70

mV drive activating transitions of E–C coupling, whereas the negative-going pulses drive transitions between inactivated states of the voltage sensor.

DISCUSSION

In this paper and the previous one (Brum *et al.* 1988) we report inhibitory effects of extracellular solutions with low $[Ca^{2+}]$ on the flux of Ca^{2+} release from the sarcoplasmic reticulum and on intramembrane charge movement. There is plenty of evidence in these reports that both effects are causally related.

The effect on intramembrane charge movement has two aspects; as shown in the first sections of this paper, the charge that moves at voltages positive to the usual holding potential of -100 or -90 mV becomes less in low $[Ca^{2+}]_o$. Additionally, a modified procedure permits the demonstration of charge movements during hyperpolarizing pulses. These charge movements increase in low $[Ca^{2+}]_o$ and become so obvious that the conventional method of charge measurement no longer works.

We believe that the effects demonstrated in Fig. 2 and Table 1 are most simply explained by the co-existence of two types of charge which interconvert and are affected differently by low $[Ca^{2+}]_o$. A simple model of the voltage sensor and its relationship with Ca^{2+} release is introduced in the next section. The model explains qualitatively most observations in these papers.

A four-state model of intramembrane charge

To explain their observations on the distribution of intramembrane charge in depolarized fibres, Brum & Ríos (1987) recently introduced the following state model of intramembrane charge movement, generally similar to a model of Bezanilla, Taylor & Fernández (1982) for Na^+ channel gating currents. In a depolarized fibre most particles ('voltage sensors') are in the inactivated states; charge 2, which is defined operationally as the charge that is measured in the fibres at $V_H = 0$ mV, arises at transitions between the inactivated states. The distribution of charge 2 is known in detail, it is centred at about -115 mV and its apparent valency (derived from the slope of the distribution) is about 1 (Brum & Ríos, 1987).

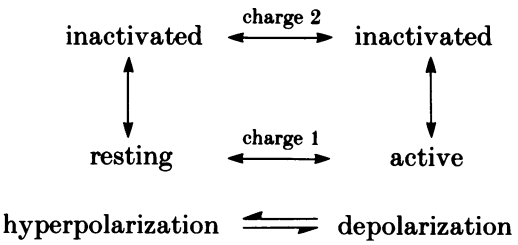

In polarized fibres ($V_H = -100$ mV) charge moves with pulses that would cause little or no charge movement at $V_H = 0$ mV. Specifically, in polarized fibres, pulses from -70 to 0 mV move most of the charge. This is explained in terms of the model as follows: the resting state becomes highly populated, depolarization drives the transition to 'active' which is accompanied by charge movement and signals the SR Ca^{2+} release channels to open. If the voltage of equal distribution of the resting →

active transition is near −30 mV, then the transition will give rise to a charge movement with the general properties of the well-studied charge of the normally polarized fibre. This charge is usually referred to as 'charge 1'; therefore, in terms of the model we *define* as charge 1 the charge mobile in the transitions between the two lower states in the diagram.

It will be shown below that it is enough to assume only the horizontal transitions in the model to be intrinsically voltage dependent (that is, producing charge movement) with very different transition voltages, to explain inactivation, that is, the spontaneous occurrence of transitions to the inactivated states when the system is held at a depolarized potential, and to explain recovery at polarized holding potentials.

In the framework of this simple model the effects of low Ca^{2+} are explained by the postulate that extracellular Ca^{2+} binds to both lower states (resting and active) with higher affinity than to the inactivated states. In qualitative terms, in normal $[Ca^{2+}]_o$ at a normal resting potential, most sensors are in the resting state and the voltage distribution of charge is close to that of the resting $\leftrightarrow$ active transition, centred at −30 mV or so; in low $[Ca^{2+}]_o$ the inactivated states are populated even at negative values of V_H; the mobile charge is partly charge 2, moving at potentials negative to −70 mV and causing a negative shift of the overall distribution of charge. As only the resting $\rightarrow$ active transition opens channels, Ca^{2+} release is inhibited.

In this version of the model, the binding site on the sensor is always accessible to extracellular Ca^{2+}, and does not change its location in the membrane field when the protein undergoes voltage-driven transitions; in other words, bound Ca^{2+} is not part of the mobile charge. A model with modified assumptions in which Ca^{2+} is part of the mobile charge is considered later.

The fact that the inhibition of Ca^{2+} release and changes in charge movement are more complete in a solution that contains neither Ca^{2+} nor Mg^{2+} implies that Mg^{2+} may substitute for Ca^{2+} at the binding site. A study of selectivity of this binding site is currently in progress in our laboratory (G. Pizarro, R. Fitts & E. Ríos, in preparation); interestingly, Na^+ can also substitute for Ca^{2+} at the modulator site, although with much lower affinity (Brum, Fitts, Pizarro & Ríos, 1987). In apparent agreement with our results Barrett & Barrett (1978) reported abolition of contractility in a solution with no Mg^{2+} or Ca^{2+}; however, their solution had a concentration of Na^+ that in our conditions is sufficient to permit E–C coupling (Brum *et al.* 1987). The discrepancy is probably related to a more depolarized holding potential in their experiments.

Given the widely separated transition voltages in the model, pulses positive to −70 mV will mainly drive movements of charge 1 whereas pulses negative to −70 mV will move mainly charge 2. This justifies the practice of referring to the charge moved by depolarizing pulses (from −70 mV) as charge 1 and the charge moved by hyperpolarizing pulses as charge 2.

Equilibrium distribution of the four-state model

Although this model proves insufficient in detailed quantitative analysis, it is so simple and has so much predictive value that we will develop it in detail. The diagram introduces a slightly different nomenclature in which the 'resting' and

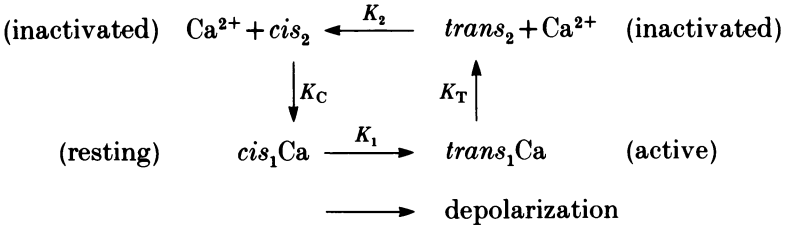

'active' states are now cis_1 and $trans_1$, *cis* (myoplasmic) and *trans* (extracellular) representing the side of the membrane in which a hypothetical positive charge would dwell to give rise to the observed charge movements. The subindices 1 and 2 refer to the type of charge associated with the transitions, charge 1 in the activating transition, charge 2 in the transitions between inactivated states. Ca^{2+} is assumed bound to the cis_1 and $trans_1$ states, at a site accessible from the extracellular medium. In this simple formulation the model is restricted to four states by assuming that cis_1 and $trans_1$ with no bound calcium are negligibly populated. This restriction is relaxed later (with no increase in complexity). The Ks represent equilibrium constants, defined always in the direction of the arrow as follows:

$$K_1 \equiv \frac{trans_1Ca}{cis_1Ca} = \exp[(V-V_1)z_1\beta], \tag{3}$$

$$K_2 \equiv \frac{cis_2}{trans_2} = \exp[-(V-V_2)z_2\beta)], \tag{4}$$

$$K_T \equiv \frac{trans_2}{trans_1Ca}, \tag{5}$$

$$K_C \equiv \frac{cis_1Ca}{cis_2}. \tag{6}$$

In these equations cis_1Ca, $trans_1Ca$, cis_2 and $trans_2$ represent fractional occupancies or probabilities. Equations (3) and (4) express the fact that the horizontal transitions are voltage dependent with centre voltages V_1 and V_2 and transfer of z_1 and z_2 elementary units of charge across the membrane electric field. $\beta \equiv e/kT \simeq 1/24$ mV where e is the elementary charge and k is Boltzmann's constant. Ca^{2+} is assumed bound to the cis_1 and $trans_1$ states.

By sequential substitution among eqns (3)–(6) and the conservation condition that all probabilities add to unity, the equilibrium concentration can be obtained as a function of voltage,

$$cis_1Ca = \{1+\exp[(V-V_1)/k_1]+K_T\exp[(V-V_1)/k_1] + K_T\exp[(V-V_1)/k_1]\exp[-(V-V_2)/k_2]\}^{-1}, \tag{7}$$

where $k_1 \equiv (z_1\beta)^{-1}$ and $k_2 \equiv (z_2\beta)^{-1}$ are the 'slope factors' of the Boltzmann distribution of charge 1 and charge 2. Analogous expressions apply to the probabilities of the other states.

Kinetics of the four-state model

When perturbed by a step change in potential, the probabilities in the four-state model relax to a new equilibrium following a time course that is the sum of three

exponentials plus a constant (equilibrium) value. These solutions are cumbersome in general (Jacquez, 1972) but can be conveniently simplified in our particular application.

In muscle the equilibrium occupancies are attained in a time scale of seconds. Fortunately, the time scale of the measured charge movements is much briefer; therefore we include in the model the assumption that the horizontal transitions are much faster (by at least one order of magnitude), than the vertical ones. This assumption simplifies the problem in the important sense of making charges 1 and 2 separable. In the brief time frame of charge movement measurements, the vertical transitions can be neglected and charges 1 and 2 considered the result of horizontal transitions proceeding in parallel, without mutual interactions. The above simplification amounts to making one of the three exponentials much slower (it applies to the processes of inactivation and repriming). The other two exponentials describe the independent movements of charge 1 and charge 2.

A practical consequence is that the distribution curve of total charge *vs.* voltage will be the sum of two Boltzmann functions, one corresponding to charge 1, the other to charge 2,

$$Q(V) = Q_{1,\max}\{1+\exp[-(V-V_1)/k_1]\}^{-1} + Q_{2,\max}\{1+\exp[-(V-V_2)/k_2]\}^{-1}. \quad (8)$$

Inactivation

Inactivation, that is, the fact that the system goes into refractory states when depolarized but not when normally polarized, is given the following explanation in the framework of the four-state model. At large positive potentials only the *trans* states are populated. The system goes to $trans_2$ spontaneously, implying that $K_T \gg 1$. Since we made the assumption that K_T is not voltage dependent, it will be greater than 1 at all voltages. Then one is left with the burden of explaining why the system does not inactivate at resting or hyperpolarized potentials.

The microscopic reversibility condition provides the answer. At hyperpolarized potentials the *cis* states will be most populated, so that $1/K_C$ will measure the tendency of the system to inactivate. In accordance with microscopic reversibility,

$$1/K_C = K_1 K_2 K_T = \exp[(V_2 - V_1)/k] K_T,$$

in which we have made the (non-essential) simplifying assumption $k_1 = k_2 = k$. If V_2 is much more negative than V_1, $\exp[(V_2 - V_1)/k]$ is much less than 1; this makes $1/K_C$, the tendency to inactivation at hyperpolarized potentials, much less than K_T, the tendency to inactivation at depolarized potentials.

In more intuitive terms, the large and negative value of the transition potential V_2 of the inactivated states implies that the cis_2 state is intrinsically unstable. Consequently, there will be a tendency towards repriming (going from cis_2 to cis_1) at potentials that populate cis_2. This is one of the most attractive features of the model, especially since the wide separation between the transition potentials V_1 and V_2, which makes repriming possible, is taken from the experimentally measured distributions of charge and not introduced *ad hoc*.

The above considerations also permit us to derive an explicit expression of the 'inactivation curve', that is the curves of Fig. 5, in which the test pulse moves most

of the available charge 1. We must calculate, in terms of the model, the amount of charge 1 available to move at a given holding potential. The maximum charge that can move in a $cis_1 \rightarrow trans_1$ transition, at any holding potential, is simply proportional to the sum of the equilibrium occupancies of both states. From eqns (7) and (3) that is:

$$cis_1\mathrm{Ca} + trans_1\mathrm{Ca} = cis_1\mathrm{Ca} + cis_1\mathrm{Ca}\exp[(V-V_1)z_1\beta]$$
$$= \{1 + K_T(1+\exp[-(V-V_2)/k_2])/(1+\exp[-(V-V_1)/k_1])\}^{-1}. \quad (9)$$

V now represents a potential maintained long enough to permit the attainment of equilibrium (holding potential).

The role of calcium. Calcium is bound to the sensor in states cis_1 and $trans_1$ only. Therefore, $[Ca^{2+}]_o$ enters the equilibrium equation through K_T: the reaction

$$trans_1\mathrm{Ca} \overset{K}{\leftrightarrow} trans_2 + Ca^{2+},$$

where K is the dissociation constant $[trans_2][Ca^{2+}]_o/[trans_1\mathrm{Ca}]$, has its equilibrium ratio determined by $[Ca^{2+}]_o$,

$$K_T \equiv \frac{trans_2}{trans_1\mathrm{Ca}} = \frac{K}{[Ca^{2+}]_o}. \quad (10)$$

Figure 12 compares the quantitative predictions of the model with the actual measurements. Figure 12*A* represents two experimental Q *vs.* V curves: the circles are average values of charge in the fibre of Figs 1, 2 and 3 (average 'on' and 'off' except for hyperpolarizing pulses where, as discussed before, only the 'off' areas were plotted). The squares are values of charge in a fibre held depolarized ($V_H = 0$ mV). Its distribution of charge is very close to the average distribution in depolarized fibres (Brum & Ríos, 1987). The charges were normalized to their maximum values (52 nC/μF at $V_H = -100$ mV and 44 nC/μF at $V_H = 0$ mV). The continuous curves were generated with eqn (8) and the parameters $V_1 = -26$ mV, $V_2 = -115$ mV and $k_1 = k_2 = 15$ mV. $Q_{1,\max}$ is large in the normally polarized case (0·92) and small in the depolarized situation (0·12). These values for $Q_{1,\max}$ were obtained from the next set of computations.

Figure 12*B* represents inactivation curves in two different $[Ca^{2+}]_o$. The experimental values are averages and error bars obtained from Fig. 5 (open symbols for reference solution, filled symbols for low Ca^{2+}). The continuous curves were generated with eqn (9), the values given above for V_1, V_2, k_1 and k_2, and $K_T = 8$ in reference $[Ca^{2+}]_o$ and 40 in low $[Ca^{2+}]_o$. From eqn (9) with these parameters, $Q_{1,\max}$ and $Q_{2,\max}$ were calculated as needed to compute the curves in Fig. 12*A*. In summary, all curves in Fig. 12*A* and *B* were generated from the model and one choice of five free parameters.

By making $k_1 = k_2$ we are assuming that the apparent valency of the mobile charge is the same in both voltage-dependent transitions; consequently, the Q *vs.* V curves in Fig. 12 were normalized to the maximum charge, and indications (Fig. 9, Table 1) that the changes in charge 1 are greater than the opposite changes in charge 2 were ignored. We feel that the quality of the data at the high voltages needed to reach saturation of charge 1 is insufficient to determine the maximum of Q_1; the assumption $k_1 = k_2$ is made here as a first approximation.

It may be seen that this simple model, with four states and six free parameters,

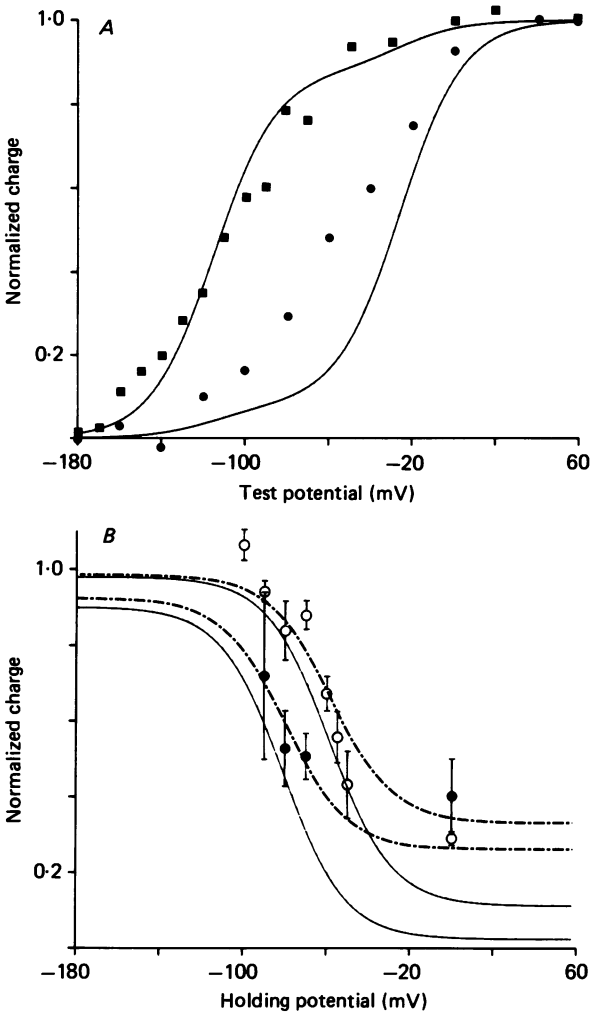

Fig. 12. Simulations with a four-state model. *A*, curves of charge *vs.* test pulse voltage at a holding potential of 0 mV (left-side curve) and −100 mV (right-side curve). The curves were calculated with text eqn (8) and the parameters $V_1 = -26$ mV, $V_2 = -115$ mV, $k_1 = k_2 = 15$ mV, $Q_{1,\max} = 0{\cdot}12$ (left) and 0·92 (right). ■, charge moved as a function of voltage at a holding potential of 0 mV. Only 'off' areas used. Values normalized to the maximum charge moved (44 nC/μF). Fibre 258, diameter 60·5 μM; linear capacitance 6·04 nF. Temperature, 10 °C, reference solution. ●, charge moved in a fibre held at −100 mV; same fibre and records as in Figs 2 and 3. The charges were normalized to the maximum (52 nC/μF) obtained as sum of the maximum charge during positive-going pulses plus the maximum moved by hyperpolarizing pulses. *B*, continuous lines are inactivation curves generated with eqn (9). V_1, V_2, k_1 and k_2 same as in *A*. $K_T = 8$ in reference solution (right-side curve) and 40 in low $[Ca^{2+}]_o$ (left-side curve). Dashed curves ($Z(V)$) are related to the continuous curves ($Y(V)$) by the transformation: $Z(V) = 0{\cdot}75\ Y(V) + 0{\cdot}25$. Same data as in Fig. 5. ○, average of experimental values in reference solution. ●, averages from same fibres in 10 μM-Ca^{2+}. Bars, ±S.E.M.

accounts qualitatively for the main observations. It accounts for the sharply different distribution of charge in polarized and depolarized fibres, it gives the approximate shape and location of the inactivation curves, and it predicts a shift to the left of the inactivation curves in low Ca^{2+} by 22 mV. Kinetic aspects of the model will be explored in the next section.

Some deficiencies of the model are readily apparent; perhaps the most obvious is, in Fig. 12*B*, the existence of a large fraction of charge that does not disappear at a holding potential of 0 mV. Our recent experiments with the Ca^{2+} antagonist nifedipine (Ríos & Brum, 1986, 1987) analogously show that the drug may block essentially all Ca^{2+} release but always spares about 25% of the charge that moves between −70 and 0 mV. A simple assumption is that there are components of charge movement not related to the E–C coupling process that do not inactivate and are not accounted for in this description. With this *ad hoc* assumption (0·25 of the total charge independent of the holding potential), the dashed curves are generated.

It is interesting to note that the four-state model, in the assumption $k_1 = k_2$, gives a sound rationale to the form of the function used to fit the inactivation curve (eqn (1)). Indeed, eqn (1) has the form of a constant term plus a 'Boltzmann' (two-state canonical distribution) function with negative slope,

$$Q(V) = A + B\{1 + \exp[(V - \bar{V})/k]\}^{-1}, \tag{11}$$

where A and B are constants.

By equating the second members in eqns (9) and (11) and solving for A, B and $\bar{V}$ it can be proved that the theoretical inactivation function (9) predicted by the model has the same form as (11). In particular $\bar{V}$, the half-inactivation voltage, is

$$\bar{V}/k = \ln \frac{\exp(V_1/k) + K_T \exp(V_2/k)}{1 + K_T}. \tag{12}$$

Thus, $\bar{V}$ is a logarithmic mean of V_1 and V_2 with weights 1 and K_T. When K_T is very large, as is the case in low $[Ca^{2+}]_0$ (eqn (10)), the half-inactivation voltage moves close to V_2.

Kinetics of charge immobilization

In the framework of the present model charge immobilization is a misnomer. Indeed, the disappearance of charge 1 corresponds to the depopulation of cis_1 and $trans_1$, and it is accompanied by increased probability of the inactivated states and increase in charge 2. The totally different voltage distribution of charge 2 explains the disappearance of charge movement in the voltage range above −70 mV and appearance of charge movement in a more negative range. For this reason, the term 'charge mutation', understood as disappearance of one type of charge and appearance of another, is preferable.

The time course of inactivation corresponds, in terms of the model, to passage of sensors from $trans_1$Ca to $trans_2$ (at depolarized potentials the other inactivating transition, cis_1Ca to cis_2, will not contribute significantly as cis_1Ca will have low probability). The kinetics of inactivation are again simplified by the assumption that the horizontal transitions are much faster; they may be assumed in equilibrium during inactivation. If k_{21} and k_{12} are the unidirectional rate constants of the $trans_1\text{Ca} \rightarrow trans_2$ transition, the time constant of inactivation will be $(k_{21} + k_{12})^{-1}$. If,

as written in the diagram, inactivation includes dissociation of Ca^{2+} which is lost to the extracellular medium, the rate of the backward reaction will be proportional to $[Ca^{2+}]_o$

$$trans_1 Ca \underset{k_{12}}{\overset{k_{21}}{\rightleftharpoons}} trans_2 + Ca^{2+},$$

the rate constant of inactivation will be

$$k_{21} + [Ca^{2+}]_o k_{12}. \tag{13}$$

This is in conflict with the experimental observation that the rate of inactivation decreases when $[Ca^{2+}]_o$ increases (Fig. 6).

A simple modification of the model, which permits it to keep its desirable equilibrium properties while changing its kinetics to agree with the observations, is represented in the diagram:

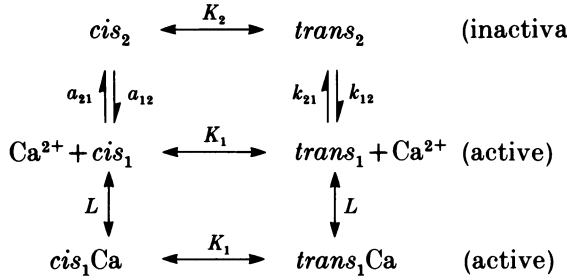

where

$$L \equiv [trans_1][Ca^{2+}]/[trans_1 Ca]. \tag{14}$$

In this version the $trans_1 \rightleftharpoons trans_2$ transition is rate limiting, whereas the reactions involving Ca^{2+} are in equilibrium in the time scale of inactivation.

In this case the differential equation determining inactivation is

$$d(cis_2 + trans_2)/dt = -k_{12}\, trans_2 + k_{21}\, trans_1. \tag{15}$$

The complete kinetic solution of this problem is given in the Appendix. The kinetics of inactivation as explored with large conditioning pulses constitute a simple case of the general solution in which the voltage is high, so that all horizontal transitions are sufficiently displaced to the right that only the three *trans* states have to be considered. From eqns (14) and (15) and a conservation relation, the inactivation process is found to be exponential with rate constant,

$$k_{12} + k_{21}\, L/([Ca^{2+}]_o + L). \tag{16}$$

Considering that k_{12} must be small if inactivation proceeds to essential completion as observed, eqn (16) implies that the rate constant of inactivation will be inversely proportional to $[Ca^{2+}]_o$ when $[Ca^{2+}]_o$ is large.

The addition of two states as described does not change the equilibrium properties of the four-state model because

$$\frac{trans_1}{cis_1} = \frac{trans_1 Ca}{cis_1 Ca} = \frac{trans_1 + trans_1 Ca}{cis_1 + cis_1 Ca} = K_1. \tag{17}$$

Thus, the states $trans_1$ and $trans_1 Ca$ can be considered as one for equilibrium

computation purposes, as well as cis_1 and cis_1Ca. This simplification makes the equilibrium equations isomorphic to those of the four-state model.

Kinetics of repriming

The term repriming refers in general to the recovery of E–C coupling functions that occurs upon repolarization of a fibre previously inactivated by sustained depolarization. Brum & Ríos (1987) showed that repriming includes recovery of charge 1 and decrease of charge 2. These two changes of opposite sign were approximately cotemporal, with time constants of about 35 s at 10 °C.

In two recent communications (Brum, Ríos & Goldman, 1985; Pizarro, Fitts, Brum, Rodríguez & Ríos, 1987) we have shown that the extent of repriming at a given holding potential is extremely sensitive to $[Ca^{2+}]_o$ but the time constant of repriming is not. These properties are qualitatively accounted for by the model. After the fibre has been equilibrated at 0 mV the model predicts that only state $trans_2$ will be significantly occupied. Accordingly, upon repolarization, the states significantly occupied will be those in the diagram. The transitions governed by K_2 and L will be in equilibrium; the rate of repriming, determined by the rate constants k_{12} and k_{21}, will be trivially independent of $[Ca^{2+}]_o$ as k_{12} and k_{21} are independent of $[Ca^{2+}]_o$.

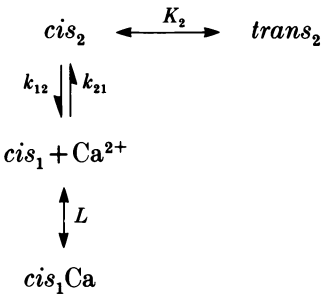

The extent of repriming will be a function of $[Ca^{2+}]_o$ as higher $[Ca^{2+}]_o$ tends to drive the reaction towards the cis_1Ca form, favouring the repriming process.

Other aspects of charge movement

This model accounts qualitatively for most observations reported in this paper, the preceding one (Brum *et al.* 1988) and the studies of charge 2 of Brum & Ríos (1987). The model also predicts the existence of subthreshold charge (Schneider, Ríos & Kovács, 1981; Rakowski, Best & James-Kracke, 1985; Melzer, Schneider, Simon & Szücs, 1986), as essentially all of charge 2 moves at potentials lower than the threshold for Ca^{2+} release. However, the model fails to explain the fact, first shown by Schneider *et al.* (1981), that at least part of the subthreshold charge has to move before release can start, suggesting the existence of at least two closed states in a sequence leading to the active state:

$$\text{resting} \rightarrow \text{resting}' \rightarrow \text{active}.$$

This model was recently shown by Melzer *et al.* (1986) to predict correctly the relationship between charge and Ca^{2+} release in conditions that did not significantly populate inactivated states. The model of Melzer *et al.* (1986) and our present model

thus provide alternative views of subthreshold charge as occurring respectively in series and in parallel with the charge that signals Ca^{2+} release. It is likely that a more complicated model, with several states in the horizontal (voltage-dependent) direction, as well as the vertical transitions proposed here, will be necessary to fully reproduce the observations.

Two recent communications are directly relevant to the present results and model: Lamb (1987) did not find a reduction in charge 2 described by Brum & Ríos (1987) upon changing from a depolarized to a negatively polarized holding potential and did not find an increase in charge 2 in the presence of nifedipine as shown by Ríos & Brum (1987). By contrast, Melzer & Pohl (1987) did confirm the result, finding moreover that the Ca^{2+} antagonist D600 increased charge 2 in normally polarized fibres, a result also obtained by Fill, Fitts, Pizarro & Ríos (1987). A possible reason for the discrepancies is that the fibres in Lamb's experiments show little non-linear charge after repolarization; as indicated in that paper, the charge movement that would be measured with conventional controls (-20 mV pulses from -90 mV) can be derived by integration of the differential plots presented. If this is done for example in Fig. 9 of Lamb (1987), which summarizes the results in that paper, it is found that the charge goes through a maximum of 7·5 nC/μF (at 10 mV) and drops at higher voltages; this is only 15–25% of maximum charges measured conventionally in mammalian muscle (Hollingworth & Marshall, 1981; Simon & Beam, 1985). The low extracellular free Ca^{2+} or the high intracellular Na^+ in the experiments of Lamb (1987) might be reasons for the large difference. In spite of these major discrepancies regarding the fate of charge 2 upon polarization, all these papers constitute evidence of the existence of non-linear charge movement in the control currents used in the conventional methods, as pointed out by Brum & Ríos (1987). This problem warrants the search for alternative controls; those defined by Brum & Ríos (1987) seem to avoid the problems of the conventional ones even though they have their own set of problems, as discussed in Methods.

Effects of Ca^{2+} channel antagonists

Ca^{2+} blocking agents such as D600 (Eisenberg, McCarthy & Milton, 1983; Berwe *et al.* 1986; Melzer & Pohl, 1987; Fill *et al.* 1987; Fill, 1987), D890 (Donaldson, Dunn & Huetteman, 1984) and nifedipine (Ríos & Brum, 1987) are now recognized to be antagonists of E–C coupling (they prevent contraction and Ca^{2+} release). Regarding intramembrane charge, they decrease charge 1 (Hui *et al.* 1984; Lamb, 1986; Ríos & Brum, 1986, 1987; Melzer & Pohl, 1987) and increase charge 2 (Ríos & Brum, 1986, 1987; Melzer & Pohl, 1987) in the same way as prolonged depolarization (Brum & Ríos, 1987) or low $[Ca^{2+}]_o$ do (this paper).

The present model provides a straightforward explanation of the effect of Ca^{2+} antagonists. They would bind to the sensors and lower their affinity for Ca^{2+}, in fact stabilizing the inactivated states. The concept is represented in the diagram.

This scheme predicts that: (a) Ca^{2+} antagonists (represented by N) will favour inactivation of Ca^{2+} release, a prediction consistent with observations of Eisenberg *et al.* (1983) and Ríos & Brum (1986, 1987); (b) Ca^{2+}antagonist action will be favoured by prolonged depolarization because the inactivated states become more populated (consistent with observations of Ríos & Brum, 1986, 1987); (c) they will decrease charge 1 (cf. Hui *et al.* 1984; Lamb, 1986; Ríos & Brum, 1987; Melzer &

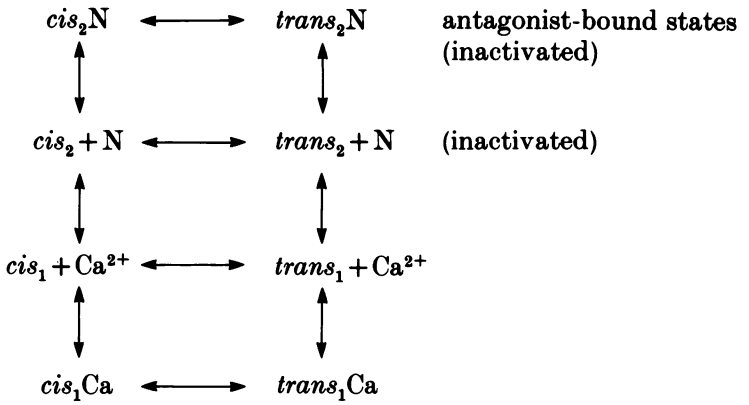

Pohl, 1987), and increase charge 2 (Ríos & Brum, 1987; Melzer & Pohl, 1987); (d) they will prevent repriming (as observed by Curtis & Eisenberg, 1985; and Fill, 1987); (e) their action will be antagonized by hyperpolarization (as reported by Berwe *et al.* 1987); (f) their action will be favoured by low $[Ca^{2+}]_0$ and antagonized by high $[Ca^{2+}]_0$ (as reported by Ríos, Brum & Stéfani, 1986; Ríos & Brum, 1986). Independent and compelling arguments for Ca^{2+} antagonist drugs binding to the inactivated (and not the active) states of the sensor have been presented by Fill (1987) based on his experiments with nisoldipine on skinned fibres.

Potentiation by a conditioning depolarization

One way of explaining the apparent potentiation of charge movement by a conditioning depolarization (Figs 6 and 7) is as an effect of the increase in intracellular Ca^{2+} caused by the conditioning pulse; Ca^{2+} could bind to an intracellular modulator site and promote the states associated with charge 1. Lüttgau, Gottschalk & Berwe (1986) and Berwe *et al.* (1986) have discussed models of the voltage sensor that include an intracellular Ca^{2+} binding modulator site.

This site could be envisioned as distinct from the extracellular binding site explored in the present work; alternatively it could be the same site. In this hypothesis the binding site would face the intracellular medium at rest and would be driven to the luminal side upon depolarization.

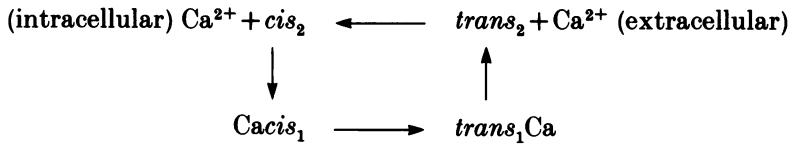

In this version Ca^{2+} would contribute part of the mobile charge. This model is thus related to the one recently proposed by Graf & Schatzmann (1984) to explain effects of low Ca^{2+} on mammalian muscle contractility. A striking consequence of the above diagram (in which it departs radically from the model of Graf & Schatzmann) is that, under the conditions of the experiments of Figs 6 and 7, the voltage sensor would be working as a carrier of Ca^{2+} and causing net outward flux of the ion. Current work in our laboratory tests the specific predictions of various forms of such carrier models.

The voltage sensor of E–C coupling

Since the initial description of intramembrane charge movement, evidence has accumulated that relates it causally to Ca^{2+} release from the SR (Chandler *et al.* 1976; Horowicz & Schneider, 1981*b*; Kovács, Ríos & Schneider, 1979; Schneider *et al.* 1981; Hui *et al.* 1984; Melzer *et al.* 1986; Rakowski *et al.* 1986; Ríos & Brum, 1987). However, the evidence remains circumstantial, the charge movement molecules have not been isolated, identified or localized and the mechanism of signalling remains disputable. Additionally, the existence of various components of charge has been proposed on the basis of kinetic dissections and pharmacological effects. The problem with these dissections is that they are not unique; thus, the existing estimates of Q_γ (Adrian & Peres, 1979; Hui, 1983) are widely different, and similar uncertainties exist regarding charge 2 (or Q_α). These difficulties have led Caillé, Ildefonse & Rougier (1985) to question the whole concept that charge movement signals Ca^{2+} release.

This paper and the preceding one demonstrate parallel changes, of similar magnitude, co-temporal, and covering at least one order of magnitude, in both charge movement and Ca^{2+} release. They must be considered together with the demonstration by Melzer *et al.* (1986) of a linear relationship between Ca^{2+} release and charge moved with different pulses, the demonstration by Pizarro *et al.* (1987) of co-temporal repriming of charge 1, Ca^{2+} release and disappearance of charge 2, the demonstration of parallel, linearly related changes of Ca^{2+} release and charge movement in fibres exposed to nifedipine (Ríos & Brum, 1987), observations of Hui *et al.* (1984) on fibres paralysed by D600, and of Csernoch, Kovács & Szücs (1987) on the potentiation of E–C coupling by perchlorate. All these results now form a wide body of data showing proportional and co-temporal changes in charge and Ca^{2+} release. The fact that most of the charge (here defined as charge 1) varies in parallel with Ca^{2+} release, suggests that not a minor part but most of it is involved in the signalling process and unequivocally localizes charge movement at the voltage sensor of E–C coupling.

APPENDIX

Slow transients in a six-state model

The purpose of this Appendix is to derive the rate constant of relaxation of the model represented in the diagram. In this model, the transitions between states $trans_1$ and $trans_2$ and between cis_1 and cis_2 are assumed rate limiting and all others are assumed fast by comparison.

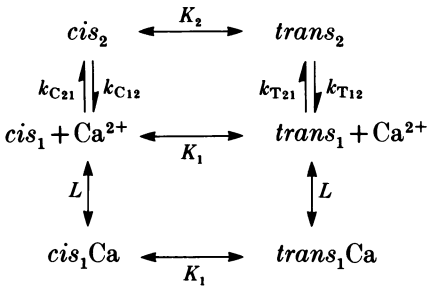

The equations of equilibrium are:

$$trans_1 = K_1 cis_1, \tag{A 1}$$

$$cis_2 = K_2 trans_2, \tag{A 2}$$

$$cis_1\mathrm{Ca} = cis_1\ \mathrm{Ca}^{2+}/L, \tag{A 3}$$

$$trans_1\mathrm{Ca} = trans_1\ \mathrm{Ca}^{2+}/L, \tag{A 4}$$

where $\mathrm{Ca}^{2+} \equiv [\mathrm{Ca}^{2+}]_o$.

There is a conservation equation,

$$cis_1 + cis_2 + trans_1 + trans_2 + cis_1\mathrm{Ca} + trans_1\mathrm{Ca} = 1, \tag{A 5}$$

a single differential equation

$$\mathrm{d}(cis_2 + trans_2) = k_{C21}\, cis_1 + k_{T21}\, trans_1 - k_{C12}\, cis_2 - k_{T12}\, trans_2, \tag{A 6}$$

and an equation of microscopic reversibility,

$$k_{C21} = k_{C12} K_1 K_2 k_{T21}/k_{T12}. \tag{A 7}$$

By suitable substitutions, eqn (A 6) may be written in terms of $trans_2$ only

$$\begin{aligned}(K_2+1)\,\mathrm{d}\,trans_2/\mathrm{d}t = {} & (k_{T21}K_1 + k_{C21}) : [(1+K_1)(1+\mathrm{Ca}^{2+}/L)] - \\ & trans_2\{(1+K_2)(k_{T21}K_1 + k_{C21}) : [(1+K_1)(1+\mathrm{Ca}^{2+}/L)] + k_{T12} + k_{C12}K_2\}.\end{aligned} \tag{A 8}$$

From eqn (A 8) it follows that the rate constant of inactivation κ (that is, of appearance of states $trans_2$ and cis_2) is:

$$\kappa = (k_{T21}K_1 + k_{C21}) : [(1+K_1)(1+\mathrm{Ca}^{2+}/L)] + (k_{T12} + k_{C12}K_2)/(1+K_2). \tag{A 9}$$

When V is positive, K_1 is large and K_2 very small,

$$\kappa \simeq k_{T21}/(1+\mathrm{Ca}^{2+}/L) + k_{T12}, \tag{A 10}$$

which is the same as text eqn (16).

As eqn (A 9) is general, it also applies to the repriming process. At the negative potentials that cause repriming, K_1 is very small; K_2 is close to 1 and strongly voltage dependent. (A 9) simplifies to

$$\kappa \simeq k_{C21}/(1+\mathrm{Ca}^{2+}/L) + (k_{T12} + k_{C12}K_2)/(1+K_2). \tag{A 11}$$

From the considerations on microscopic reversibility made in the text $k_{C12} \gg k_{T12}$ and k_{C21}. Therefore, the expression (A 11) is dominated by its last term, i.e.

$$\kappa \simeq k_{C12}\frac{K_2}{1+K_2}. \tag{A 12}$$

This equation expresses a strong dependence of the rate constant of repriming on K_2, which in turn depends on the holding potential (eqn (4)).

We are grateful to Drs F. Cohen, T. DeCoursey and R. S. Eisenberg for their many comments and suggestions (in particular, the term 'charge mutation' was suggested by R. S. Eisenberg); to Dr Ted Begenisich for discussion on state models; to Dr Mónica Rodríguez for help in various stages of this work; to Ms Lucille Vaughn for careful typing. This work was funded by NIH grants AR32808 and AR07575.

REFERENCES

ADRIAN, R. H. & PERES, A. (1979). Charge movement and membrane capacity in frog muscle. *Journal of Physiology* **289**, 83–97.

ARMSTRONG, C. & BENZANILLA, F. (1977). Inactivation of the sodium channel. II. Gating current experiments. *Journal of General Physiology* **70**, 567–590.

BARRETT, J. N. & BARRETT, E. F. (1978) Excitation–contraction coupling in skeletal muscle: blockade by high extracellular concentrations of calcium buffers. *Science* **200**, 1270–1272.

BERWE, D., GOTTSCHALK, G. & LÜTTGAU, H. C. H. (1987). The effects of the Ca-antagonist gallopamil (D600) upon excitation–contraction coupling in toe muscles of the frog. *Journal of Physiology* **385**, 693–708.

BEZANILLA, F., TAYLOR, R. E. & FERNÁNDEZ, J. M. (1982). Distribution and kinetics of membrane polarization. I. Long term inactivation of gating currents. *Journal of General Physiology* **79**, 21–40.

BRUM, G., FITTS, E., PIZARRO, G. & RÍOS, E. (1987). A Ca–Mg–Na site must be occupied for intramembrane charge movement and Ca release in frog skeletal muscle. *Biophysical Journal* **51**, 552a.

BRUM, G. & RÍOS, E. (1986). Intramembrane charge movements in non-polarized skeletal muscle fibres. Inactivation without immobilization. *Biophysical Journal* **49**, 13a.

BRUM, G. & RÍOS, E. (1987). Intramembrane charge movement in skeletal muscle fibres. Properties of charge 2. *Journal of Physiology* **387**, 489–517.

BRUM, G., RÍOS, E. & GOLDMAN, J. (1985). Calcium release and charge movement in skeletal muscle fibres exposed to zero Ca and long depolarizations. *Biophysical Journal* **47**, 134a.

BRUM, G., RÍOS, E. & STÉFANI, E. (1988). Effects of extracellular calcium on the calcium movements of excitation–contraction coupling in frog skeletal muscle fibres. *Journal of Physiology* **398**, 441–473.

CAILLÉ, J., ILDEFONSE, M. & ROUGIER, O. (1985). Excitation–contraction coupling in skeletal muscle. *Progress in Biophysics and Molecular Biology* **46**, 185–239.

CHANDLER, W. K., RAKOWSKI, R. F. & SCHNEIDER, M. F. (1976). Effects of glycerol treatment and maintained depolarization on charge movement in skeletal muscle. *Journal of Physiology* **254**, 285–316.

CSERNOCH, L., KOVÁCS, L. & SZÜCS, G. (1987). Perchlorate and the relationship between charge movement and contractile activation in frog skeletal muscle fibres. *Journal of Physiology* **390**, 213–227.

CURTIS, B. A. & EISENBERG, R. S. (1985). Calcium in flux in contracting and paralyzed frog twitch muscle fibers. *Journal of General Physiology* **85**, 383–408.

DONALDSON, S. K., DUNN, R. & HUETTEMANN, D. (1984). Peeled mammalian skeletal muscle fibres: reversible block of Cl^- induced tension transients by D-600 and D-890. *Biophysical Journal* **45**, 40a.

EISENBERG, R. S., MCCARTHY, R. T. & MILTON, R. L. (1983). Paralysis of frog skeletal muscle fibres by the calcium antagonist D600. *Journal of Physiology* **341**, 495–505.

FILL, D. M. (1987). Excitation–contraction coupling: The effect of calcium channel antagonistic drugs on reprimed and inactivated skinned skeletal muscle fibres. Ph.D. Thesis. University of Illinois at Urbana, U.S.A.

FILL, D. M., FITTS, R., PIZARRO, G. & RÍOS, E. (1987). Effects of D-600 on charge movement, Ca release and Ca currents in skeletal muscle fibres. *Journal of General Physiology* (in the Press).

GRAF, F. & SCHATZMANN, H. J. (1984). Some effects of removal of external calcium on pig striated muscle. *Journal of Physiology* **349**, 1–13.

HOLLINGWORTH, S. & MARSHALL, M. W. (1981). A comparative study of charge movement in rat and frog skeletal muscle fibres. *Journal of Physiology* **321**, 563–602.

HOROWICZ, P. & SCHNEIDER, M. F. (1981*a*). Membrane charge movement in contracting and non-contracting skeletal muscle fibres. *Journal of Physiology* **314**, 565–593.

HOROWICZ, P. & SCHNEIDER, M. F. (1981*b*). Membrane charge moved at contraction thresholds in skeletal muscle fibres. *Journal of Physiology* **314**, 595–633.

HUI, C. S. (1983). Differential properties of two charge components in frog skeletal muscle. *Journal of Physiology* **337**, 531–552.

HUI, C. S., MILTON, R. L. & EISENBERG, R. S. (1984). Charge movement in skeletal muscle fibres

paralyzed by the calcium-entry blocker D-600. *Proceedings of the National Academy of Science of the U.S.A.* **81**, 2582–2585.

JACQUEZ, J. A. (1972). In *Compartmental Analysis in Biology and Medicine*, pp. 44–49. Amsterdam: Elsevier.

KOVÁCS, L., RÍOS, E. & SCHNEIDER, M. F. (1979). Calcium transients and intramembrane charge movement in skeletal muscle fibres. *Nature* **279**, 391–396.

LAMB, G. (1986). Components of charge movement in rabbit skeletal muscle. The effects of tetracaine and nifedipine. *Journal of Physiology* **376**, 85–100.

LAMB, G. D. (1987). Asymmetric charge movement in polarized and depolarized muscle fibres of the rabbit. *Journal of Physiology* **383**, 349–368.

LÜTTGAU, H. C., GOTTSCHALK, G. & BERWE, D. (1986). The role of Ca^{2+} in inactivation and paralysis of excitation–contraction coupling in skeletal muscle. *Progress in Zoology* **33**, 195–203.

LÜTTGAU, H. C., GOTTSCHALK, G. & BERWE, D. (1987). The effect of calcium and Ca-antagonists upon excitation–contraction coupling. *Canadian Journal of Physiology and Pharmacology* **65**, 717–723.

LÜTTGAU, H. C. & SPIECKER, W. (1979). The effects of calcium deprivation upon mechanical and electrophysiological parameters in skeletal muscle fibres of the frog. *Journal of Physiology* **296**, 411–429.

MCLAUGHLIN, S. G. A. (1977). Electrostatic potentials at membrane–solution interfaces. In *Current Topics in Membrane Transport*, ed. BRONNER, F. & KLEINZELLER, A., vol. 9, pp. 71–144. New York: Academic Press.

MCLAUGHLIN, S. G. A., SZABO, G. & EISENMAN, G. (1971). Divalent ions and the surface potential of charged phospholipid membranes. *Journal of General Physiology* **58**, 667–687.

MELZER, W. & POHL, B. (1987). Effects of D600 on the voltage sensor for Ca release in skeletal muscle fibres of the frog. *Journal of Physiology* **390**, 151*P*.

MELZER, W., RÍOS, E. & SCHNEIDER, M. F. (1984). Time course of calcium release and removal in skeletal muscle fibres. *Biophysical Journal* **45**, 637–641.

MELZER, W., RÍOS, E. & SCHNEIDER, M. F. (1987). A general procedure for determining calcium release in skeletal muscle fibers. *Biophysical Journal* **51**, 849–863.

MELZER, W., SCHNEIDER, M. F., SIMON, B. & SZÜCS, G. (1986). Intramembrane charge movement and Ca release in frog skeletal muscle. *Journal of Physiology* **373**, 481–511.

PIZARRO, G., FITTS, R., BRUM, G., RODRÍGUEZ, M. & RÍOS, E. (1987). Simultaneous recovery of charge movement and Ca release in skeletal muscle. *Biophysical Journal* **51**, 101a.

RAKOWSKI, R. F., BEST, P. M. & JAMES-KRACKE, M. R. (1985). Voltage dependence of membrane charge movement and calcium release in frog skeletal muscle fibres. *Journal of Muscle Research and Cell Motility* **6**, 403–433.

RÍOS, E. & BRUM, G. (1986). Nifedipine and the voltage sensor of skeletal muscle excitation–contraction coupling. *Journal of General Physiology* **88**, 50a.

RÍOS, E. & BRUM, G. (1987). A possible role of dihydropyridine receptor molecules in excitation–contraction coupling. *Nature* **325**, 717–720.

RÍOS, R., BRUM, G. & STÉFANI, E. (1986). E–C coupling effects of interventions that reduce slow Ca current suggest a role of T-tubule Ca channels in skeletal muscle function. *Biophysical Journal* **49**, 13a.

SCHNEIDER, M. F. & CHANDLER, W. K. (1973). Voltage dependent charge movement in skeletal muscle: a possible step in excitation–contraction coupling. *Nature* **242**, 244–246.

SCHNEIDER, M. F., RÍOS, E. & KOVÁCS, L. (1981). Calcium transients and intramembrane charge movement in skeletal muscle. In *The Regulation of Muscle Contraction: Excitation–Contraction Coupling*, ed. GRINNELL, A. D. & BRAZIER, M. A. B., pp. 131–141. New York: Academic Press.

SIMON, B. J. & BEAM, K. G. (1985). Slow charge movement in mammalian skeletal muscle. *Journal of General Physiology* **85**, 1–20.

WINKLER, R. L. & HAYS, W. L. (1975). *Statistics: Probability, Interference and Decision*, 2nd edn. New York: Holt, Rinehart and Winston.